Visible Light Sensitive Photocatalyst, Delafossite Structured α-$AgGaO_2$

Yoshihiko Maruyama,[†] Hiroshi Irie,*[,†] and Kazuhito Hashimoto*[,†,‡]

Department of Applied Chemistry, The University of Tokyo, 7-3-1 Hongo, Bunkyo-ku, Tokyo 113-8656, Japan, and Research Center for Advanced Science and Technology (RCAST), The University of Tokyo, 4-6-1 Komaba, Meguro-ku, Tokyo 153-8904, Japan

Received: June 1, 2006; In Final Form: August 17, 2006

Delafossite structured α-$AgGaO_2$ powder was successfully synthesized through a cation exchange reaction. α-$AgGaO_2$ has a band gap of 2.4 eV, absorbs visible light up to 520 nm, and effectively decomposes 2-propanol to CO_2 via acetone by irradiating with either UV light (300−400 nm) or visible light (420−530 nm). The values of the quantum efficiency are similar (ca. 0.6%) under light irradiations with wavelengths of 365, 390, 430, 470, and 510 ± 10 nm, but steeply decrease with wavelengths longer than 530 ± 10 nm, which support a 2.4 eV band gap. In contrast, the other polymorph, β-$AgGaO_2$ powder, which has a band gap of 2.1 eV, shows a negligible activity when irradiating with either UV light or visible light. The higher oxidation activity of α-$AgGaO_2$ is probably due to its larger band gap, which is formed at the top of its valence band in a lower energy region as compared to β-$AgGaO_2$. Moreover, the first-principle calculations of α-$AgGaO_2$ and β-$AgGaO_2$ clearly indicate that α-$AgGaO_2$ has a remarkably larger dispersed valence band as compared to β-$AgGaO_2$, which is advantageous to the photocatalytic activity due to the efficient hole conduction.

Introduction

In addition to the recent increasing interest in the photocatalytic applications for environmental purification, visible light sensitive photocatalysts are necessary to efficiently utilize solar energy and indoor light. Thus, numerous studies have investigated these photocatalysts. Typically, UV-active photocatalysts are modified by anion doping,[1−5] metal doping,[6−8] and generating oxygen deficiency.[9] However, such dopants and oxygen vacancies act as charge recombination centers. Therefore, these methods are disadvantageous to the photocatalytic activity. Another common method is to produce photocatalysts with smaller band gap energies without dopants by forming the maximums of their valence bands in the higher energy region. These photocatalysts have been intensely investigated, especially in the field of photocatalytic water splitting with specific d^{10}/$d^{10}s^2$ metal ions (Ag^+,[10,11] In^{3+},[12−14] Bi^{3+},[15] etc.), but there are limited reports in the field of photooxidation of organic compounds.[16,17]

Delafossite structured oxides, which are denoted by ABO_2 and include d^{10} metal ions (Cu^+ or Ag^+), are successful materials for p-type transparent conductors (TCO) due to their structural advantages.[18−20] Figure 1a and b shows the crystal structures of delafossite structured oxides. Delafossite has a layered structure, which can be further classified into two polytypes, 3R (Figure 1a) and 2H (Figure 1b). Although the stacking patterns of the layers differ slightly, both materials can be regarded as the delafossite structure. The O−A−O dumbbell bonding layers are interleaved with edge-sharing BO_6 octahedra blocks along the *c*-axis. These O−A−O layers and BO_6 layers act as separate conduction paths for holes and electrons, respectively.[18] In addition, each oxygen atom builds an OB_3A tetrahedron, forming an O-2sp^3 orbital, which does not form localized O2p nonbonding states.[19,20] These tetrahedra are favorable for hole conduction. Furthermore, a small repulsion

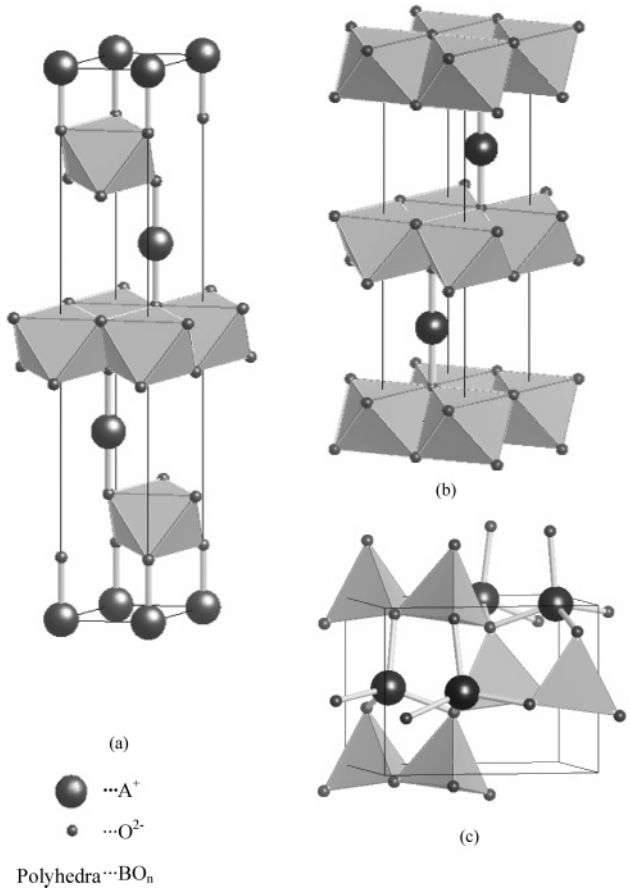

Figure 1. (a) Delafossite structure (3R-type), (b) delafossite structure (2H-type), and (c) β-$NaFeO_2$ structure.

* Corresponding author. Tel.: +81-3-5452-5080. Fax: +81-3-5452-6593. E-mail: irie-hrs@light.t.u-tokyo.ac.jp (H.I.); hashimoto@light.t.u-tokyo.ac.jp (K.H.).
† Department of Applied Chemistry.
‡ RCAST.

10.1021/jp063406s CCC: $33.50
Published on Web 10/24/2006

between O^{2-} ions in two-coordinated O−A−O dumbbell bonds causes a short A−O bonding. The interaction between the A^+ and O^{2-} ions then becomes stronger,[21] and a highly dispersed valence band structure is expected. This highly dispersed valence band leads to a small effective mass of the holes with a higher hole mobility. In contrast to the strong interactions between them, interactions between the A^+ ions are weak because they work mainly through $A^+-O^{2-}-B^{3+}-O^{2-}-A^+$ links, which are two-dimensional in delafossite oxides. These weak and low-dimensional interactions between the A^+ ions induce a band gap, which is bigger than that of A_2O hemioxides.[19,20] These structural features, which are related to the effective hole conduction and relatively large band gaps, are advantageous to the p-type conductivity, transparency, and photocatalytic activity.

Copper delafossite oxides, $CuMO_2$ (M = Al, Cr, Fe, Ga, Y, In, etc.), have been reported as p-type semiconductors without doping,[19,23,24] but most of them were black[22,23] with small indirect band gaps (1.26−1.65 eV).[24] Hence, $CuMO_2$ should have an insufficient power to photooxidize organic compounds. Among silver delafossite oxides ($AgMO_2$), $AgInO_2$ powder is orange,[22,23] indicating that the band gap is too narrow to generate photooxidative activity to decompose organic compounds. However, $AgAlO_2$ powder is light gray.[25] The gray color implies that there is a relatively larger band gap, which can absorb UV light, because the gray color should originate from the oxygen vacancies. Therefore, we selected delafossite type $AgGaO_2$, that is, α-$AgGaO_2$,[26] because it should have an adequate band gap to absorb visible light and to produce the photocatalytic activity. In this report, we used α-$AgGaO_2$ to investigate the photooxidation of organic compounds.[27] Because $AgGaO_2$ has another polymolph, that is, β-$NaFeO_2$-type β-phase (Figure 1c), we also examined the β-$AgGaO_2$ phase.

Experimental Section

α-$AgGaO_2$ powder was prepared by a cation exchange reaction.[21,28,29] $NaGaO_2$ powder was initially synthesized by a solid-state reaction. Commercial Na_2CO_3 (Wako Chemical, 99.5%) and Ga_2O_3 (Kojundo Chemical, 99.9%) powders were used as the starting materials. Stoichiometric amounts of the starting materials for $NaGaO_2$ were wet ball milled using ZrO_2 balls as the milling medium in polyethylene bottles. The resulting mixture was calcined at 700 °C for 5 h. The obtained powder was reground and sintered at 900 °C for 5 h to produce white β-$NaGaO_2$ powder. β-$NaGaO_2$ then was mixed with $AgNO_3$ (Wako Chemical, 99.8%) and KNO_3 (Wako Chemical, 99%) with a molar ratio of 1:1.03:1 in an agate mortar, followed by heating at 210 °C in air for 24 h. KNO_3 was used to lower the mixing enthalpy of the molten nitrates to accelerate the substitution of Na^+ by Ag^+.[21] The resulting powder was pulverized and washed with enough distilled water to remove the remaining nitrates, and dried in a refrigerator. The obtained powder was β-$AgGaO_2$, which was further heated in water at 60−70 °C for 12 h to complete the delafossite phase, α-$AgGaO_2$.

The crystal structures of the prepared powders were identified by X-ray diffraction (XRD; Spectris, Panarytical PW-1700). The surface areas were determined by BET (Micrometrics, TriStar3000). The diffuse reflectance spectra were obtained with a UV−vis spectrometer (Rigaku, UV2550). The grain sizes of the powders were observed by scanning electron microscopy (SEM; S-4200, Hitachi Ltd.).

The photocatalytic oxidation activities were evaluated by the decomposition of gaseous 2-propanol (IPA) while irradiating with light. Each 300 mg powder sample was uniformly spread in a lab dish (irradiation area was 5.5 cm^2) and placed in a 500 mL glass vessel with a quartz-made lid. The atmosphere in the vessel then was substituted with dry synthetic air. A 300 ppm (300 ppmv, that is, 6.7 μmol) concentration of the reactant gas (IPA) was injected into the vessel and stored in the dark. After the IPA concentration was confirmed constant, light irradiation was initiated. IPA was photocatalytically oxidized via acetone or directly into CO_2 and H_2O.[30] To evaluate the photocatalytic activity, the amounts of IPA, acetone, and CO_2 were monitored by a gas chromatograph (Shimadsu, GC-8A) equipped with CO_2-methanizer (Shimadsu, MTN-1). UV light with wavelengths between 300 and 400 nm and visible light between 420 and 530 nm were achieved by a Xe lamp (Hayashi Tokei, Luminar Ace 210) using a glass filter (Asahi-Technoglass, UV-D36B) and a combination of three glass filters (Asahi-Technoglass, B-47, Y-44, C-40C), respectively. The experiments were performed on α-$AgGaO_2$, β-$AgGaO_2$, and commercial anatase TiO_2 nanoparticles (Ishihara Sangyo, ST-01). The light intensities for the visible and UV lights were adjusted to 1000 and 750 μW cm^{-2}, respectively, to equalize the absorbed photon numbers (9.6×10^{14} quanta cm^{-2} s^{-1}) in the presence of α-$AgGaO_2$. Table 1 summarizes the absorbed photon numbers. Additionally, IPA decomposition in the presence of α-$AgGaO_2$ was measured under monochromatic lights to observe the wavelength-dependence of the quantum efficiency (QE is the same as the photonic efficiency) using a Czerny-Turner type monochromator (Ritsu Ouyou Kogaku, MC-10N) and either a Xe lamp or a Hg−Xe lamp (Hayashi Tokei, Luminar Ace 100). The widths of the monochromatic lights were approximately 20 nm. Higher order diffracted lights were cutoff with the appropriate glass filter. Table 2 summarizes the intensities, wavelengths, and absorbed photon numbers.

TABLE 1: Absorbed Photon Numbers of Light Irradiation on α-$AgGaO_2$[a]

	α-$AgGaO_2$	β-$AgGaO_2$	TiO_2 (anatase)
visible light (λ = 420−530 nm, 1000 μW cm^{-2})	9.6×10^{14}	2.2×10^{15}	−[b]
UV light (λ = 300−400 nm, 750 μW cm^{-2}	9.6×10^{14}	1.3×10^{15}	9.2×10^{14}

[a] Absorbed photon number/quanta cm^{-2} s^{-1}. [b] Absorbed photon number could not be determined for TiO_2 (anatase) because its absorption in the visible light region was virtually zero.

The QE calculations were conducted using the same procedure as previously reported.[2,17] The initial acetone and CO_2 generation rates by IPA decomposition were calculated using the conventional least-squares method. Only one photon participated in the decomposition process of IPA to acetone.[30] Therefore, the QE values for acetone generation were calculated using the following equation: $QE_{acetone}$ = initial acetone generation rate/absorption rate of incident photon. As compared to the mechanism for acetone generation, the mechanism for CO_2 generation is complex. Therefore, it is difficult to determine the number of photons participating in the reaction because there are two reaction paths. Assuming the following formula, $C_3H_8O + 5H_2O + 18H^+ \rightarrow 3CO_2 + 18H^+$, that is, six photons are required to produce one CO_2 molecule, the QE values for CO_2 generation were calculated using the following equation, QE_{CO_2} = 6 × initial CO_2 generation rate/absorption rate of incident photon.

Plane-wave-based density functional method calculations were carried out for α- and β-$AgGaO_2$ by employing an ab initio

TABLE 2: Intensities and Absorbed Photon Numbers of Monochromatic Light Irradiation on α-$AgGaO_2$

wavelength/nm	365	390	430	470	510	530	550	570
intensity/μW cm^{-2}	80[a]	100	100	100	100	100	100	100
absorbed photon number/ quanta cm^{-2} s^{-1}	1.0×10^{14}	1.2×10^{14}	1.1×10^{14}	9.6×10^{13}	8.7×10^{13}	8.9×10^{13}	9.3×10^{13}	9.7×10^{13}

[a] Hg−Xe lamp was used as a light source.

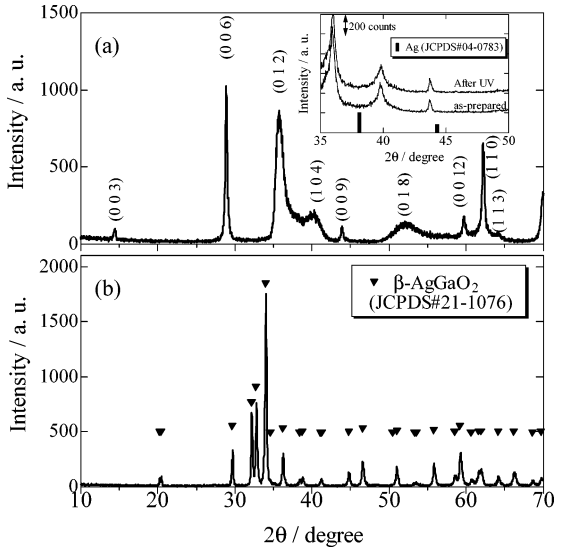

Figure 2. X-ray powder diffraction patterns of (a) α-$AgGaO_2$ and (b) β-$AgGaO_2$. The inset of (a) indicates no changes in XRD profiles for α-$AgGaO_2$ between before and after 72 h UV light (the same UV light condition in Table 1) irradiation.

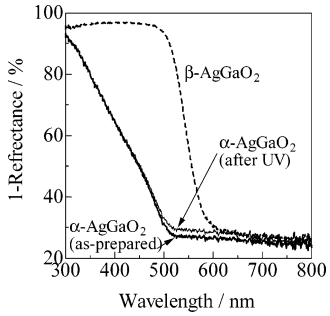

Figure 3. UV−vis absorption spectra of α-$AgGaO_2$ and β-$AgGaO_2$.

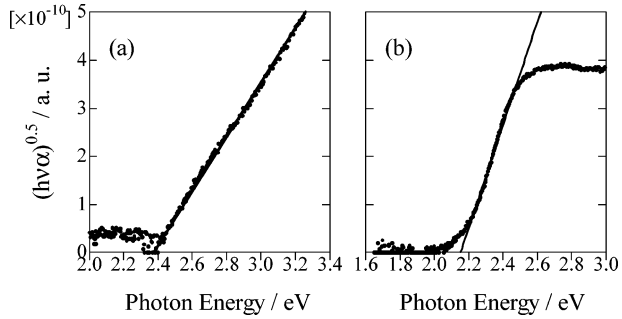

Figure 4. $(h\nu\alpha)^{1/2}$ plot for (a) α-$AgGaO_2$ and (b) β-$AgGaO_2$. The absorption coefficient α is estimated by the Kubelka−Munk conversion of reflectance.

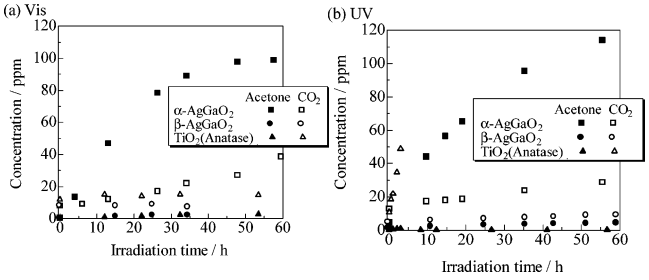

Figure 5. Changes in acetone and CO_2 concentrations by IPA decomposition as a function of time in the presence of α-$AgGaO_2$ or β-$AgGaO_2$ or TiO_2 (anatase) under (a) visible light ($420 < \lambda < 530$ nm) and (b) UV light ($300 < \lambda < 400$ nm).

total energy and molecular dynamics program, VASP (Vienna Ab initio Simulation Program).[31,32] The wave functions and potentials of the core orbitals were replaced by a projector augmented wave (PAW) by Blöchl,[33] and the exchange-correlation energy was calculated by the generalized gradient approximation (GGA). At first, the lattice structures of α- and β-$AgGaO_2$ were optimized for their atomic positions using lattice parameters[22,34] reported for related structures. The kinetic energy cutoff was 500 eV for structure optimization. The density of states (DOSs) and band structures were calculated from the optimized structures with an energy cutoff of 400 eV.

Result and Discussion

α-$AgGaO_2$ and β-$AgGaO_2$ were obtained as yellow and orange powders, respectively. Figure 2a and b shows the XRD patterns of the obtained α- and β-$AgGaO_2$ samples, respectively. Both samples show homogeneous crystalline α- and β-$AgGaO_2$ phases. α-$AgGaO_2$ is mainly the 3R delafossite phase. Peak broadenings are observed only in Figure 2a when the peaks were diffracted from crystallographic planes neither perpendicular nor horizontal to the *c*-axis, which is attributed to the long-range stacking disorder between the 2H and 3R polytypes along the *c*-axis.[35] The surface areas of α- and β-$AgGaO_2$ are 2.80 and 1.49 m^2 g^{-1}, respectively. According to the SEM observations, both are agglomerated and have similar powder sizes of 200−1000 nm (not shown here). β-$AgGaO_2$ is shaped into spherical particle, but α-$AgGaO_2$ is shaped into hexagonal platelets, which is consistent with the previous report.[22] Figure 3 shows the UV−visible absorption spectra of α- and β-$AgGaO_2$. Both types of $AgGaO_2$ absorb in the visible light range, but the wavelength for the absorption-edge of α-$AgGaO_2$ is shorter than that of β-$AgGaO_2$. The constant absorption is larger than a wavelength of approximately 520 nm for α-$AgGaO_2$ and approximately 600 nm for β-$AgGaO_2$. The reason for the constant absorption is unclear, but may be due to the oxygen vacancies; it is well-known that the oxygen vacancy level is just below the conduction minimum in the forbidden band, which results in the absorption in a longer wavelength region.[9] Delafossite structured oxides are regarded as indirect gap semiconductors,[36−38] and the band gap of the α-$AgGaO_2$ is estimated from the tangent lines in the plots of the square root of the Kubelka−Munk functions against the photon energy as shown in Figure 4a. The tangent line extrapolated to $\alpha^{1/2} = 0$ indicates that the band gap of α-$AgGaO_2$ is 2.4 eV. Similarly, that of β-$AgGaO_2$ is 2.1 eV, as shown in Figure 4b.[39]

Figure 5a and b shows the photocatalytic activity in the presence of α-$AgGaO_2$, β-$AgGaO_2$, and anatase powders while irradiating with UV (300−400 nm) and visible light (420−530 nm), respectively. The anatase powder shows a photocatalytic activity under UV light irradiation to produce acetone and CO_2, but did not display a photocatalytic activity under visible light

irradiation. The increases in the acetone and CO_2 concentrations under both visible or UV light irradiation were negligible in the presence of β-$AgGaO_2$, which confirms β-$AgGaO_2$ does not have photocatalytic activity. On the contrary, in the presence of α-$AgGaO_2$ under either light irradiation, the acetone and CO_2 concentrations increased by decomposing IPA. Judging from the fwhm (full width at half-maximum) of XRD patterns, the crystallinity of β-$AgGaO_2$ is higher than that of α-$AgGaO_2$ in the present samples. It means that even the lower crystallized α-$AgGaO_2$ possesses much higher photocatalytic activity than the higher crystallized β-$AgGaO_2$. Therefore, we can conclude that α-$AgGaO_2$ generally possesses much higher photocatalytic activity than the higher crystallized β-$AgGaO_2$. These results are due to the differences in the band gaps. β-$AgGaO_2$ has a smaller band gap, which forms in the top of its valence band in a higher energy region and results in an insufficient power to oxidate IPA. In contrast, α-$AgGaO_2$ has a larger band gap so that it exhibits the appropriate oxidation power. In addition to the band gap, the larger dispersed valence band of α-$AgGaO_2$ is attributed to the photocatalytic activity. The QE for IPA decomposition in the presence of α-$AgGaO_2$ was 0.35% under UV light, which was much lower than that in the presence of TiO_2 (6.0%). However, the QE of α-$AgGaO_2$ under visible light is 0.39%, which is much higher than values reported for other photocatalysts sensitive to visible light ($AgNbO_3$, GaN−ZnO solid solution, <0.1% under visible light).[40]

The stability of α-$AgGaO_2$ under UV light irradiation was confirmed using the XRD, XPS (X-ray photoemission spectroscopy, Perkin-Elmer Japan, 5600), and UV−visible spectrometer. The UV light condition was controlled to be the same as the IPA decomposition test in Figure 5b, as shown in Table 1. Even after 72 h irradiation, the XRD profile did not change, as compared to that before light irradiation, as shown in the inset of Figure 2a. XRD peaks derived from metallic Ag were not observed at all. The data are not shown here, but neither Ag3d, Ga3d, nor O1s XPS spectra were changed after UV light irradiation. The UV−visible absorption spectrum after UV light irradiation slightly changed as shown in Figure 3. After UV light irradiation, the value of 1-reflectance increased very slightly in the wavelength region larger than 500 nm, which corresponds to Ag plasmon absorption. Because the change in 1-reflectance was very small and no changes in XRD and XPS were observed, the present α-$AgGaO_2$ was quite stable under UV light condition in Table 1.

The QE values of IPA decomposition on α-$AgGaO_2$ were on the same order regardless of the irradiation light source (UV light (0.35%) and visible (0.39%) light), indicating that α-$AgGaO_2$ has a continuous valence band. This means that the visible light absorption of α-$AgGaO_2$ should be originated from an interband transfer, not from a transition from/to discrete energy levels generated by dopants, that is, anion-doped TiO_2[2,5] due to the following reason. As soon as the free charge carriers are photogenerated in a semiconductor and rapid communications between the different subband states in the valence band and conduction band are complete, then the photocarriers will occupy the lowest states in their corresponding bands (i.e., they become thermalized). The carrier temperature becomes equal to the ambient temperature and the carriers are indistinguishable, regardless of the initial state immediately occupied upon photoexcitation. That is, the excess photoenergy is dissipated as heat rather than as chemical potential. To confirm this explanation, we performed IPA decomposition on α-$AgGaO_2$ under monochromatic light irradiation. Figure 6 shows the results. When irradiating with wavelength shorter than 520 nm,

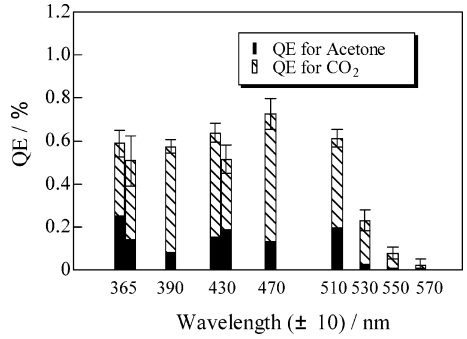

Figure 6. Dependence of the quantum efficiency (QE) on the wavelength of monochromatic light (λ = 365, 390, 430, 470, 510, 530, 550, 570 ± 10 nm). For λ = 365 and 430 nm, experiments were performed twice.

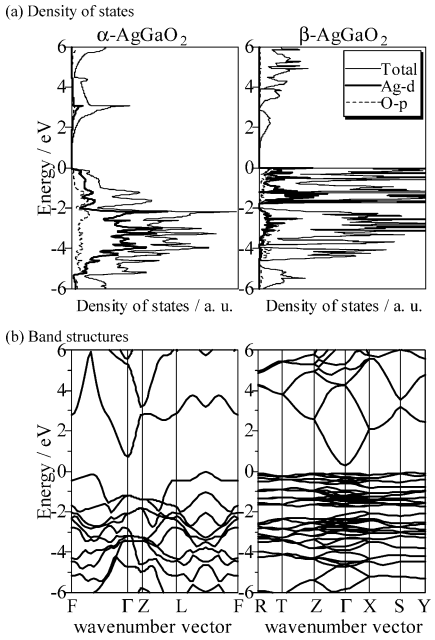

Figure 7. (a) Density of states and (b) band structures calculated for α-$AgGaO_2$ (left) and β-$AgGaO_2$ (right) using VASP.

the absorption edge and the QE values are nearly constant, but the QE values steeply decrease when irradiating with wavelengths longer than 530 ± 10 nm. These results clearly demonstrate that α-$AgGaO_2$ has a continuous band structure with a band gap of 2.4 eV.

Ab initio calculations were performed to evaluate the electronic structures of α- and β-$AgGaO_2$. Figure 7a and b shows the density of states and band structures, respectively, for α- and β-$AgGaO_2$ calculated by VASP. The valence band maximums for both α- and β-$AgGaO_2$ consist of Ag4d and O2p orbitals. Additionally, both are indirect semiconductors where an indirect transition is favorable for carrier migration. The indirect band gap of α-$AgGaO_2$ agrees well with previous reports on the electronic structures of delafossite $CuMO_2$ (M = Al, Ga, In) with a conduction band minimum on the Γ point and a valence band maximum near the F-point as calculated by the Hartree−Fock−Roothan method[36,37] or the full-potential linear augmented plane wave method.[38] As shown in Figure 7a and b, the band structures of α- and β-$AgGaO_2$ obviously differ. As expected from the structural property of delafossite oxides, the valence band of α-$AgGaO_2$ is highly dispersed, which means that the photogenerated holes have a small effective mass. This probably explains the higher photocatalytic activity in the presence of α-$AgGaO_2$ as compared to that in the presence of

β-$AgGaO_2$. In addition, the calculated band gap of α-$AgGaO_2$ is 0.73 eV, which is larger than that of β-$AgGaO_2$, 0.34 eV. This grossly underestimated band energy gap is characteristic of the density functional calculation. In α-$AgGaO_2$, the Ag−O bonds are two-coordinated and the Ag^+ ion network is two-dimensional, which lead to a large dispersion of the valence band and a sufficient band gap. However, in β-$AgGaO_2$, the Ag−O bonds are four-coordinated and the Ag^+ ion network is three-dimensional, which lead to a small dispersion of the valence band and an insufficient band gap. These results are consistent with the above studies on the structural properties and photocatalytic activities. Ag_2O has O−Ag−O dumbbell bonds similar to delafossite oxides, and the electronic structure of Ag_2O calculated by VASP has a highly dispersed valence band. However, the band gap is almost zero (not shown), which may be due to the O−Ag−O three-dimensional cross-linking as Cu_2O.[19,20] These findings are compatible with a fact that Ag_2O is a p-type semiconductor[41] with a 1.8 eV band gap, which is insufficient to photooxidize organic compounds. In contrast, silver complex-oxides, including Ag^+ ions such as $AgNbO_3$, have relatively large band gaps. However, the bonds and the interactions between the Ag^+ ion and O^{2-} ions are weak, which decrease the dispersion of the calculated valence band and lower the hole conductivity. Thus, the weak bonds and interactions may explain the low photooxidation activity of these silver complex-oxides.[42] However, α-$AgGaO_2$ is an excellent photocatalyst, which is sensitive to visible light, because it has the appropriate band gap for visible light absorption and a high hole conductivity, which both originate from its unique layered crystal structure.

Conclusion

We investigated a novel photocatalyst, which is sensitive to visible light, from the viewpoints of the electronic structure of the valence band and the crystal structure. α-$AgGaO_2$ has a relatively high photocatalytic activity and can decompose 2-propanol via acetone and ultimately produces CO_2 under visible light irradiation ($\lambda < 520$ nm). α-$AgGaO_2$ has the proper band gap energy to absorb visible light and to generate a photocatalytic activity. The calculated electronic structure of α-$AgGaO_2$ also supports that it is advantageous for the mobility of the photogenerated holes, which leads to the rather high activity. This study demonstrates that searching for a material with a delocalized and dispersed valence band by mixing a metal-d orbital with an O2p orbital is a candidate for generating a high-performance, visible light sensitive photocatalyst.

Acknowledgment. This work was supported by a Grant-in-Aid for Scientific Research on Priority Areas (417) from the Ministry of Education, Culture, Sports, Science, and Technology (MEXT) of Japan.

References and Notes

(1) Asahi, R.; Morikawa, T.; Aoki, K.; Taga, Y. *Science* **2001**, *293*, 269.
(2) Irie, H.; Watanabe, Y.; Hashimoto, K. *J. Phys. Chem. B* **2003**, *107*, 5483.
(3) Umebayashi, T.; Yamaki, T.; Tanaka, S.; Asai, K. *Chem. Lett.* **2003**, *32*, 330.
(4) Ohno, T.; Mitsui, T.; Matsumura, M. *Chem. Lett.* **2003**, *32*, 364.
(5) Irie, H.; Watanabe, Y.; Hashimoto, K. *Chem. Lett.* **2003**, *32*, 772.
(6) Borgarello, E.; Kiwi, J.; Gratzel, M.; Pelizzetti, E.; Visca, M. *J. Am. Chem. Soc.* **1982**, *104*, 2996.
(7) Sepone, N.; Hermann, J. M. *Langmuir* **1994**, *10*, 693.
(8) Choi, W.; Termin, A.; Hoffmann, M. *J. Phys. Chem.* **1994**, *97*, 13669.
(9) Nakamura, I.; Negishi, N.; Kutsuna, S.; Ihara, T.; Sugihara, S.; Takeuchi, K. *J. Mol. Catal. A* **2000**, *161*, 205.
(10) Kato, H.; Kobayashi, H.; Kudo, A. *J. Phys. Chem. B* **2002**, *106*, 12441.
(11) Konta, R.; Kato, H.; Kobayashi, H.; Kudo, A. *Phys. Chem. Chem. Phys.* **2003**, *5*, 3061.
(12) Zou, Z.; Ye, J.; Arakawa, H. *Chem. Phys. Lett.* **2000**, *332*, 271.
(13) Ye, J.; Zou, Z.; Oshikiri, A.; Matsuyama, M.; Shimoda, M.; Imai, M.; Shishido, T. *Chem. Phys. Lett.* **2000**, *356*, 221.
(14) Zou, Z.; Ye, J.; Sayama, K.; Arakawa, H. *Nature* **2001**, *414*, 625.
(15) Kudo, A.; Omori, K.; Kato, H. *J. Am. Chem. Soc.* **1999**, *121*, 11459.
(16) Tang, J.; Zou, Z.; Ye, J. *Angew. Chem.* **2004**, *116*, 4563.
(17) Murase, T.; Irie, H.; Hashimoto, K. *J. Phys. Chem. B* **2005**, *109*, 13420.
(18) Hosono, H.; Kamiya. *Bull. Ceram. Soc. Jpn.* **2003**, *38*, 825.
(19) Kawazoe, H.; Yasukawa, M.; Hyodo, H.; Kurita, M.; Yanagi, H.; Yasukawa, M.; Hosono, H. *Nature* **1997**, *389*, 939.
(20) Yanagi, H.; Kawazoe, H.; Kudo, A.; Yasukawa, M.; Hosono, H. *J. Electroceram.* **2000**, *4*, 407.
(21) Clayton, J. E.; Cann, D. P.; Ashmore, N. *Thin Solid Films* **2002**, *411*, 140.
(22) Shannon, R. D.; Rogers, D. B.; Prewitt, C. T. *Inorg. Chem.* **1974**, *10*, 713.
(23) Nagarajan, R.; Duan, N.; Jayaraj, M. K.; Li, J.; Vanagja, K. A.; Yokochi, A.; Draeseke, A.; Tate, J.; Sleight, A. W. *Int. J. Inorg. Mater.* **2001**, *3*, 265.
(24) Benko, F. A.; Koffyberg, F. P. *J. Phys. Chem. Solids* **1987**, *48*, 431.
(25) Gessner, W. *Z. Anorg. Allg. Chem.* **1967**, *352*, 145.
(26) Sheets, W. C.; Mugnier, E.; Barnabe, A.; Marks, T. J.; Poeppelmeier, K. R. *Chem. Mater.* **2006**, *18*, 7.
(27) Delafossite structured oxide photocatalysts have also been reported for $CuAlO_2$ to generate hydrogen in extreme conditions (Koriche, N.; Bouguelia, A.; Aider, A.; Trari, M. *Int. J. Hydrogen Energy* **2005**, *30*, 693) and for α-$AgAlO_2$ to degrade methylene blue (Zou, Z.; Yang, S. O.; Ye, J. *ISNEPP 2005 Abstract* **2005**).
(28) Thilo, E.; Gessner, W. *Z. Anorg. Allg. Chem.* **1966**, *347*, 151.
(29) Li, J.; Sleight, A. W. *J. Solid State Chem.* **2004**, *177*, 889.
(30) Ohko, Y.; Hashimoto, K.; Fujishima, A. *J. Phys. Chem. A* **1997**, *101*, 8057.
(31) Kresse, G.; Hafner, J. *Phys. Rev. B* **1993**, *48*, 17.
(32) Kresse, G.; Furthmüller, J. *Phys. Rev. B* **1996**, *54*, 16.
(33) Blöchl, P. E. *Phys. Rev. B* **1994**, *50*, 17953.
(34) Data from JCPDS Card, #21-1076.
(35) Jacob, A.; Parent, C.; Boutinaud, P.; Flem, G. L.; Dormerc, J. P.; Ammar, A.; Elazhari, M.; Elaatmani, M. *Solid State Commun.* **1997**, *103*, 529.
(36) Buljan, A.; Alemany, P.; Ruiz, E. *J. Phys. Chem. B* **1999**, *103*, 8060.
(37) Robertson, J.; Peacock, P. W.; Towler, M. D.; Needs, R. *Thin Solid Films* **2002**, *411*, 96.
(38) Nie, X.; Wei, S. H.; Zhang, S. B. *Phys. Rev. Lett.* **2002**, *88*, 066405.
(39) According to ab initio calculations, β-$AgGaO_2$ and α-$AgGaO_2$ are indirect semiconductors.
(40) We examined the photocatalytic activity of IPA decomposition in the presence of other visible light sensitive water-splitting photocatalysts, which have been already reported, under visible light irradiation with 10^{14}−10^{15} absorbed photon numbers. The quantum yield is 0.041% for $AgNbO_3$ (band gap $\approx$ 2.8 eV[10]) and 0.039% for a GaN−ZnO solid solution (band gap $\approx$ 2.6 eV; Maeda, K.; Tanaka, T.; Hara, M.; Saito, N.; Inoue, Y.; Kobayashi, H.; Domen, K. *J. Am. Chem. Soc.* **2005**, *127*, 8286).
(41) Fortiu, E. *Phys. Status Solidi* **1964**, *5*, 515.
(42) $AgNbO_3$ has a relatively large band gap of 2.8 eV, contains 12-coordinated long A−O bonds ($\sim$2.79 Å on average), and is considered to have weak bonds and interaction. The band structure calculated by VASP shows a larger band gap (1.68 eV) and small dispersion of the valence band, which should lead to a large effective mass and small hole conductivity.